
Modeling of Active Control on KSTAR

Oksana Katsuro-Hopkins¹, S.A. Sabbagh¹, J.M. Bialek¹, H.K. Park², J.Y. Kim³, K.-I. You³, A.H. Glasser⁴, L.L. Lao⁵



¹*Department of Applied Physics, Columbia University, New York, NY, USA*

²*Plasma Physics Laboratory, Princeton University, Princeton, NJ, USA*

³*Korea Basic Science Institute, Daejeon, Korea*

⁴*Los Alamos National Laboratory, Los Alamos, NM, USA*

⁵*General Atomics, San Diego, CA, USA*

Workshop on Active Control of MHD Stability

November 18-20, 2007

Columbia University, New York, NY

Numerical design study to optimize advanced stability of KSTAR merging present experimental results & machine design

- Motivation

- ☐ Design optimal global MHD stabilization system for KSTAR with application to future burning plasma devices

- Outline

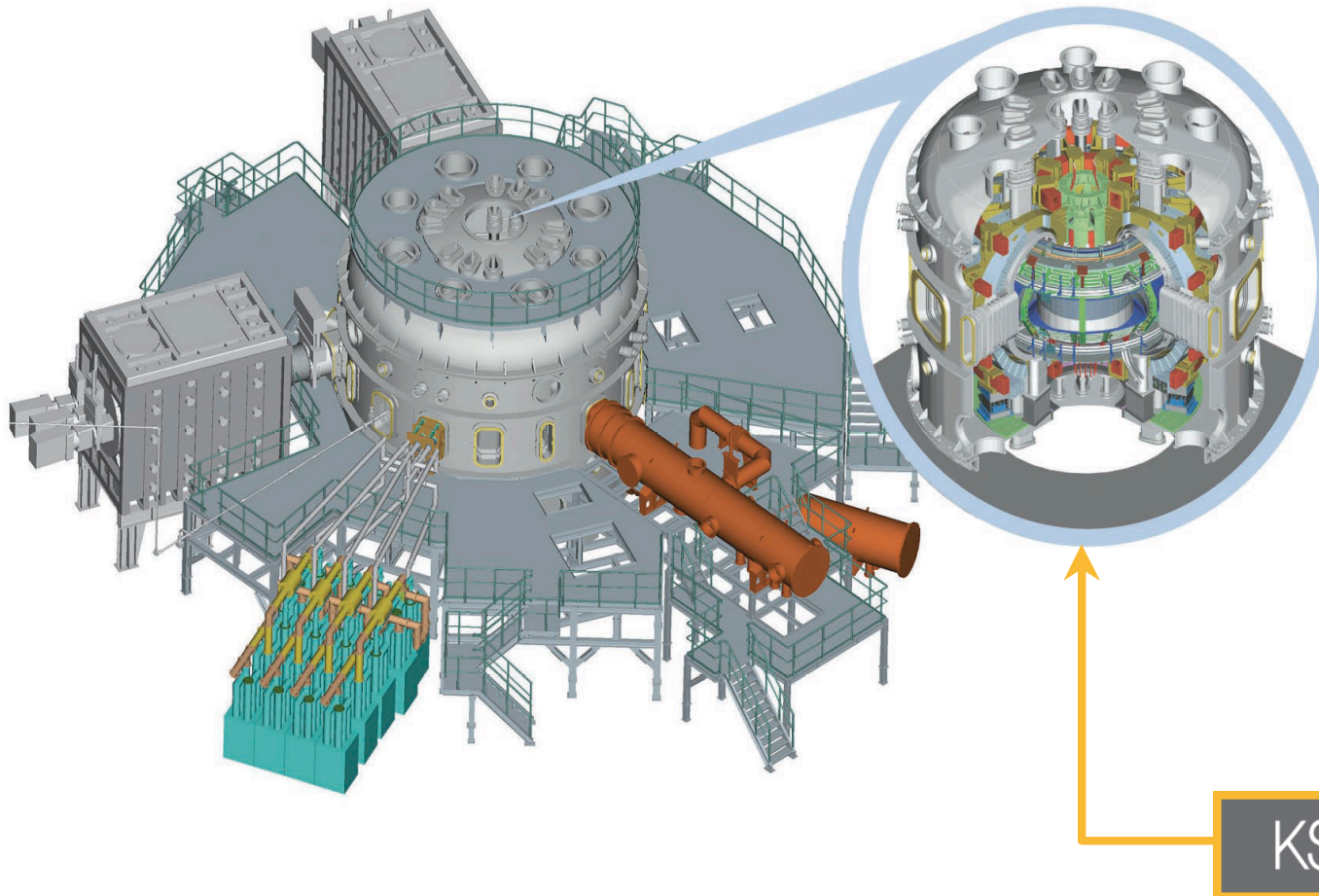
- ☐ Free boundary equilibrium calculations
- ☐ Ideal stability operational space for experimental profiles
- ☐ RWM stability and VALEN-3D modeling
- ☐ Advanced feedback control algorithm and performance

*O.Katsuro-Hopkins et al., Nucl. Fusion **47** (2007) 1157-1165.

Korea Superconducting Tokamak Advanced Research will study steady-state advanced tokamak operation & technology

Parameters:

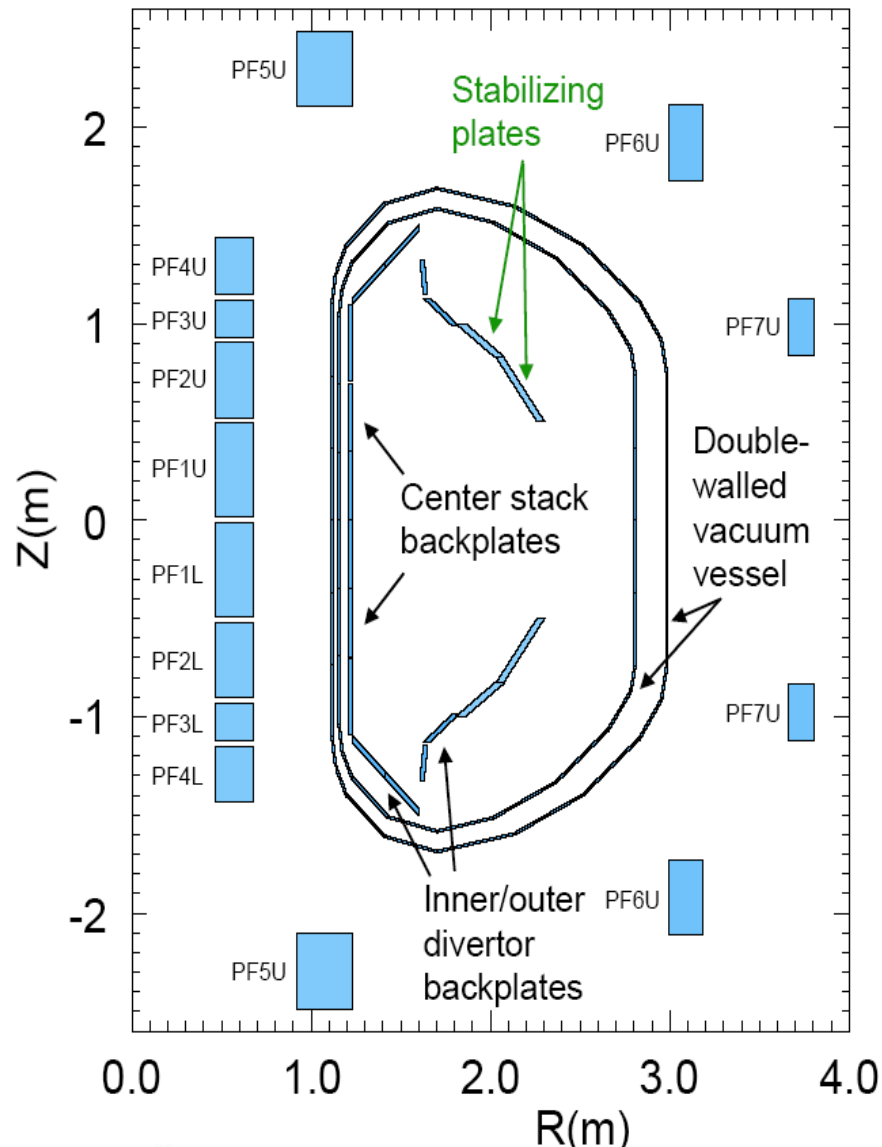
- R 1.8m
- a 0.5 m
- B_{to} 3.5 T
- τ_{pulse} 300 s
- I_p 2.0 MA
- T_i 100~300MC
- Magnet:
 - TF : Nb3Sn,
 - PF : NbTi



Free boundary equilibrium: incorporates analysis techniques used for present experiments with existing data

- Equilibrium calculations with EFIT
 - ❑ Free boundary based on machine constraint
 - ❑ Experimental (DIII-D H-mode) & generic pressure profiles
- Ideal Stability
 - ❑ DCON Kink/Ballooning Stability analysis for $n=1$ and $n=2$ modes for various wall and no-wall cases
 - ❑ Operational space in (I_i, β_n)
- RWM stability
 - ❑ Resistive Wall Mode (RWM) VALEN-3D passive/active stabilization
 - ❑ advanced control methods in the presence of sensor noise

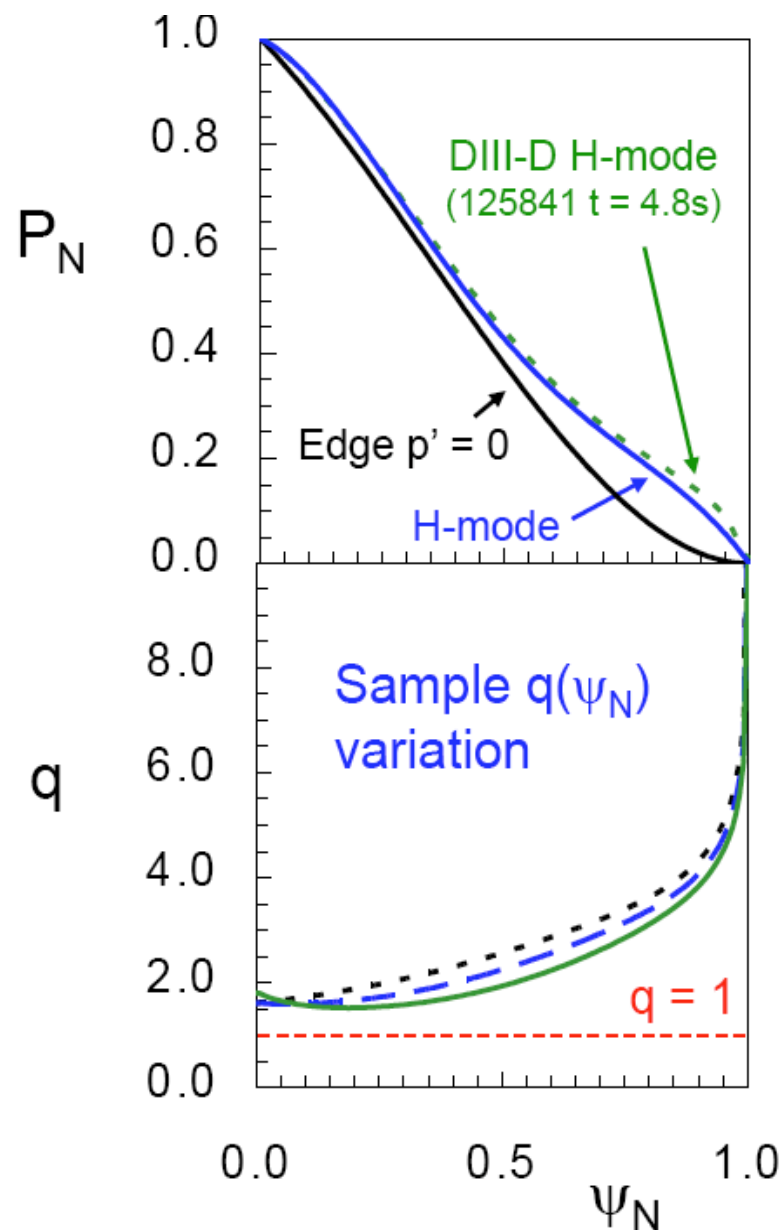
KSTAR configuration used in EFIT calculations



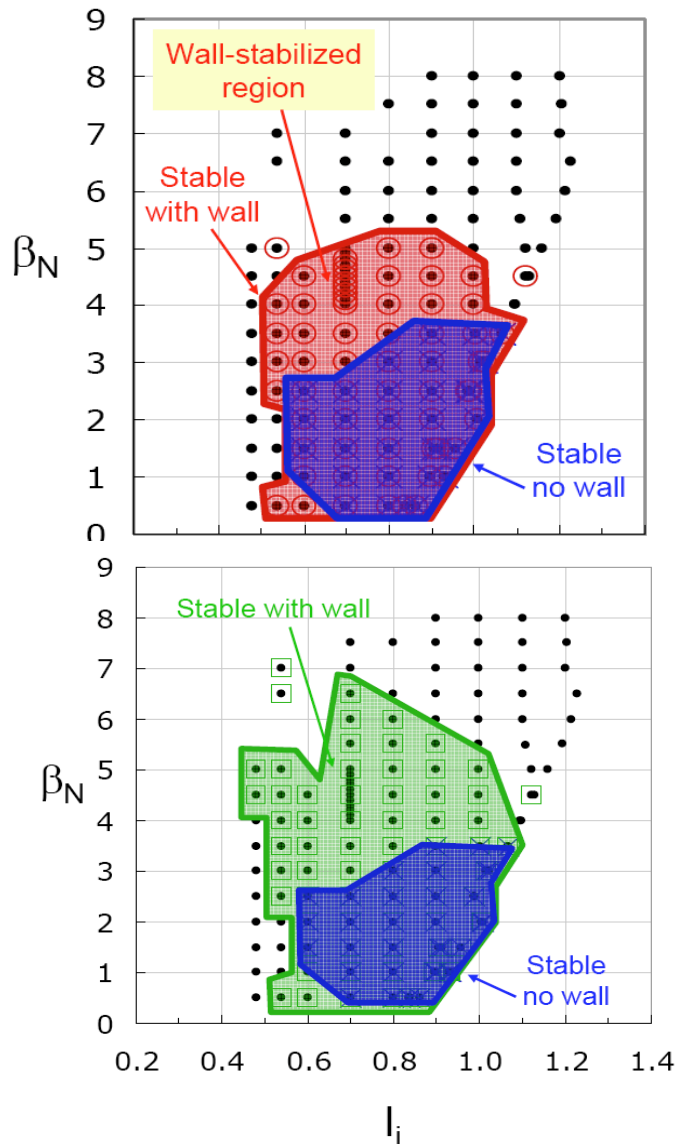
- EFIT industry-standard tool
 - Free-boundary equilibria
 - Expandable range of equilibria
- Data from KSTAR design drawings
- Passive stabilizers/vacuum vessel included.
 - Important for start up studies
 - Reconstructions during events that change edge current (e.g. ELMs)

Equilibrium variations produced to scan (I_i, β_n)

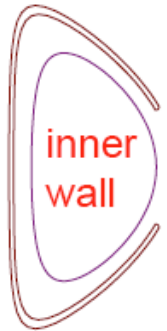
- **Boundary shape**
 - ❑ Free-boundary equilibria with high shaping $\kappa \sim 2, \delta \sim 0.8$
 - ❑ Shaping coil currents constrained to machine limits
- **Pressure profile**
 - ❑ Generic “L-mode”, edge $p' = 0$
 - ❑ H-mode, modeled from DIII-D
- **q profile**
 - ❑ Monotonic to mild shear reversal with $q_0 > 1$ and $(q_0 - q_{\min}) < 1$
- **Variations in (I_i, β_n) produced**
 - ❑ $0.5 \leq I_i \leq 1.2$; $0.5 \leq \beta_n \leq 8.0$



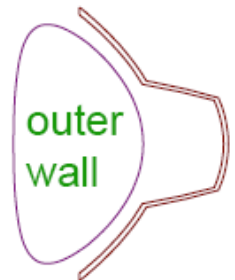
Ideal stability(DCON): conducting wall allows significant passive stabilization for n=1 H-mode pressure profile



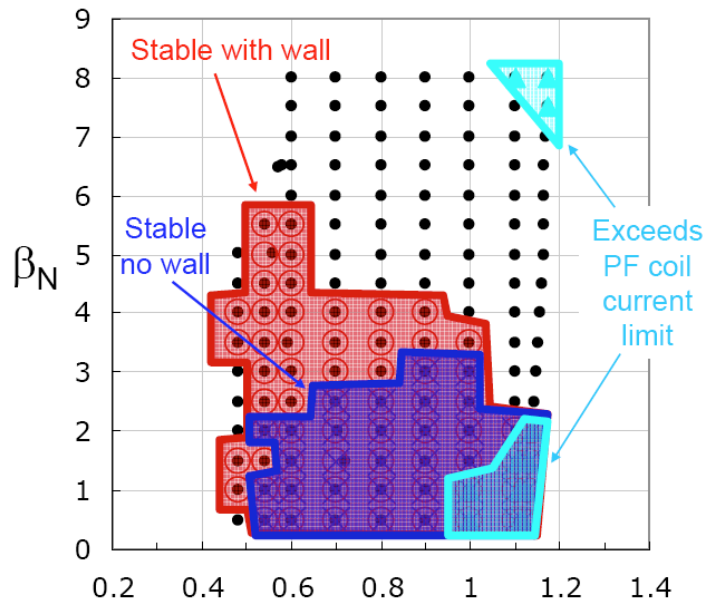
- “inner” wall used
- Wall-Stabilized β_n is a factor of two greater than for equilibrium without wall at $I_i \sim 0.7$
- Wall-Stabilized β_n from DCON agrees with VALEN-3D value



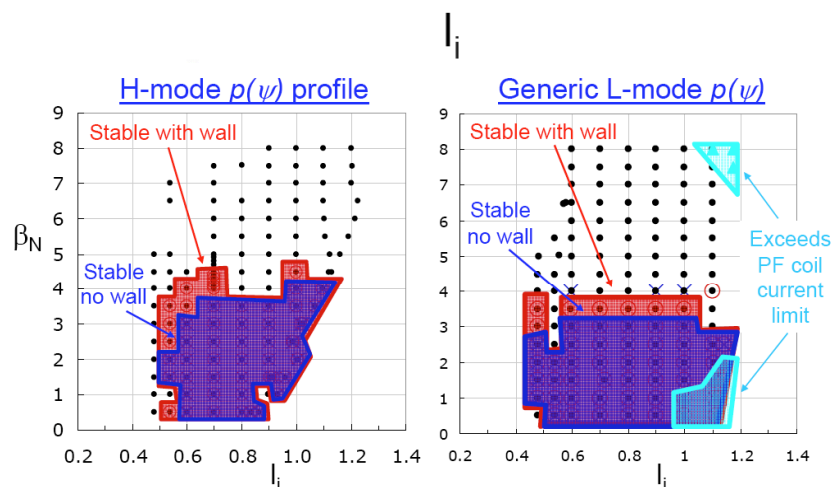
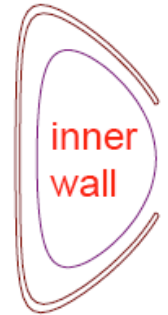
- “outer” wall used
- Wall-Stabilized $\beta_n > 6.5$ (larger than the result using “inner” wall at $I_i \sim 0.7$)
- Optimistic, but does not agree with VALEN-3D. “Inner” wall is more realistic and should be used in DCON analysis



L-mode pressure profile has large $n=1$ stabilized region



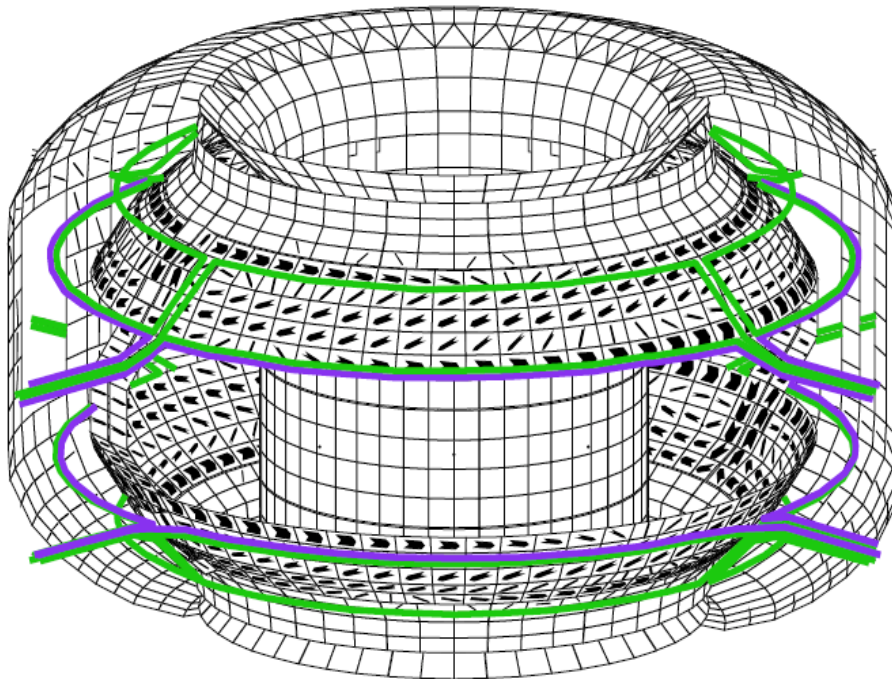
- “inner” wall used
- Wall-Stabilized region at lowest I_i (Unfavorable for $n=0$ stabilization)
- Possible difficulty to access with L-mode confinement.



- $n=2$ stability has higher no-wall & lower with-wall limits than $n=1$ for H-mode and L-mode pressure profile
 - Internal $n=2$ modes were observed in NSTX during $n=1$ active RWM stabilization.

Conducting hardware, IVCC set up in VALEN-3D* based on engineering drawings

n=1 RWM passive stabilization currents

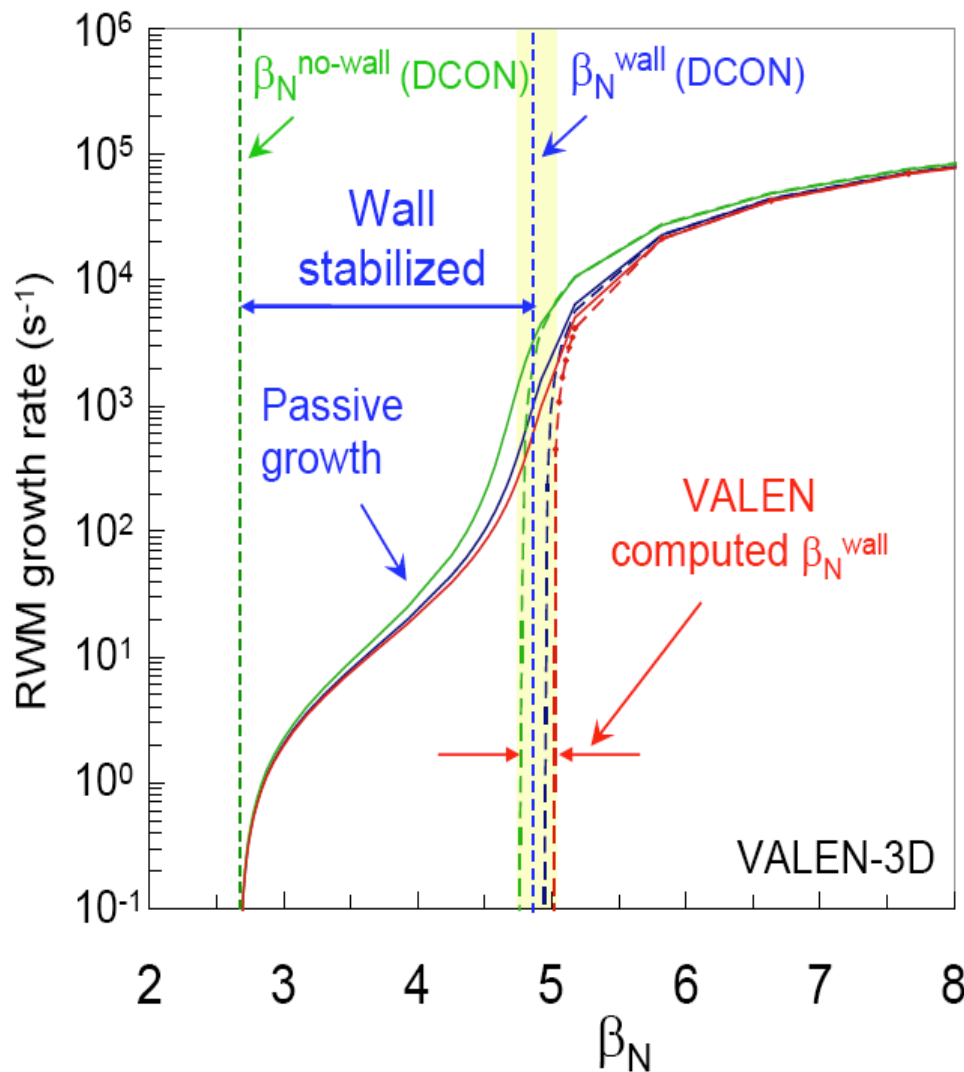


IVCC (RWM) control coils
(upper,middle,lower)

- Conducting structures modeled
 - ❑ Vacuum vessel with actual port structure
 - ❑ Center stack back-plates
 - ❑ Inner and outer divertor back-plates
 - ❑ Passive stabilizer
 - ❑ PS Current bridge
- Stabilization currents dominant in PS
 - ❑ 40 times less resistive than nearby conductors.

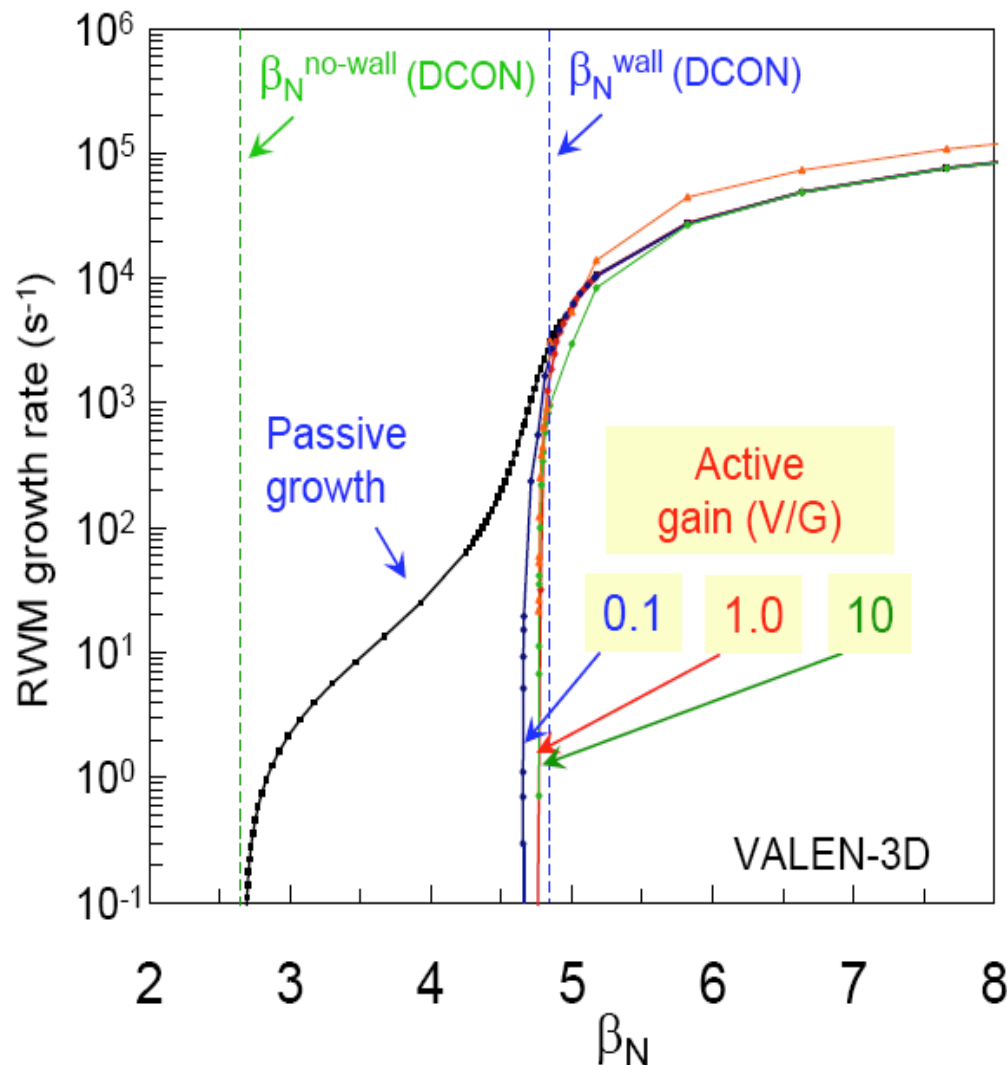
*Bialek J. et al 2001 Phys. Plasmas **8** 2170

VALEN 3-D code reproduces $n=1$ DCON β_n ideal wall limit



- Important cross-check
VALEN-3D/DCON calibration
- Equilibrium β_n scan with $I_i=0.7$
H-mode pressure profile
- DCON $n=1$ β_n limits:
 - $\beta_n^{\text{no-wall}} = 2.6$
 - $\beta_n^{\text{wall}} = 4.8$
- VALEN-3D $n = 1$ β_n^{wall}
 - $4.77 < \beta_n^{\text{wall}} < 5.0$
 - Range generated by various
RWM eigenfunctions from
equilibria near
 $\beta_n = 5$.

IVCC allows active n=1 RWM stabilization near ideal wall.



- Active n=1 RWM stabilization capability with

$$C_\beta = \frac{\beta_n - \beta_n^{\text{no wall}}}{\beta_n^{\text{wall}} - \beta_n^{\text{no wall}}} > 98\%$$

- ☐ Optimal ability for mode stabilization
- ☐ Mid-plane IVCC used
- Equilibrium β_n scan with $I_i=0.7$ H-mode pressure profile
- Computed β_n limits
 - ☐ $\beta_n^{\text{no-wall}} = 2.56$
 - ☐ $\beta_n^{\text{wall}} = 4.76$

Power estimates bracket needs for KSTAR RWM control

Proportional gain
controller

White noise (1.6-2.0G RMS)

NSTX 120047 ΔB_p sensors

(RMS values)

(RMS values)

Unloaded IVCC

$L=10\mu\text{H}$

$R=0.86\text{m}\Omega$

$L/R=12.8\text{ms}$

C_β
80%
95%

$I_{IVCC}(\text{A})$ $V_{IVCC}(\text{V})$ $P_{IVCC}(\text{W})$

30	1.6	45
41	2.0	82

$I_{IVCC}(\text{A})$ $V_{IVCC}(\text{V})$ $P_{IVCC}(\text{W})$

362	0.7	253
430	0.8	307

FAST IVCC circuit

$L=13\mu\text{H}$

$R=13.2\text{m}\Omega$

$L/R=1.0\text{ms}$

80%
95%

20.9 1.56 30.0
28.3 1.78 50.6

1.9e3 24.9 62e3
9e3 119 1.8e6

Power estimates bracket needs for KSTAR RWM control

Proportional gain
controller



LQG
controller

White noise (1.6-2.0G RMS)

NSTX 120047 ΔB_p sensors

(RMS values)

(RMS values)

Unloaded IVCC
L=10 μ H
R=0.86mOhm
L/R=12.8ms

C_β
80%
95%

I_{IVCC} (A)	V_{IVCC} (V)	P_{IVCC} (W)
30 / 29	1.6 / 0.8	45 / 24
41 / 35	2.0 / 0.9	82 / 34

I_{IVCC} (A)	V_{IVCC} (V)	P_{IVCC} (W)
362	0.7	253
430	0.8	307

FAST IVCC circuit
L=13 μ H
R=13.2mOhm
L/R=1.0ms

80%
95%

20.9	1.56	30.0
28.3	1.78	50.6

1.9e3	24.9	62e3
9e3	119	1.8e6

- Initial results using advanced Linear Quadratic Gaussian (LQG) controller yield factor of 2 power reduction for white noise.
- LQG controller consists of two steps:
 - Balanced Truncation of VALEN state-space for fixed β_n
 - Optimal controller and observer design based on the reduced order system

State-space control approach may allow superior feedback performance

- VALEN circuit equations after including plasma stability effects the fluxes at the wall, feedback coils and plasma are given by

$$\vec{\Phi}_w = \vec{L}_{ww} \cdot \vec{I}_w + \vec{L}_{wf} \cdot \vec{I}_f + \vec{L}_{wp} \cdot I_d$$

$$\vec{\Phi}_f = \vec{L}_{fw} \cdot \vec{I}_w + \vec{L}_{ff} \cdot \vec{I}_f + \vec{L}_{fp} \cdot I_d$$

$$\Phi_p = \vec{L}_{pw} \cdot \vec{I}_w + \vec{L}_{pf} \cdot \vec{I}_f + \vec{L}_{pp} \cdot I_d$$

- Equations for system evolution are given by

$$\begin{pmatrix} \vec{L}_{ww} & \vec{L}_{wf} & \vec{L}_{wp} \\ \vec{L}_{fw} & \vec{L}_{ff} & \vec{L}_{fp} \\ \vec{L}_{pw} & \vec{L}_{pf} & \vec{L}_{pp} \end{pmatrix} \cdot \frac{d}{dt} \begin{pmatrix} \vec{I}_w \\ \vec{I}_f \\ I_d \end{pmatrix} = \begin{pmatrix} \vec{R}_w & 0 & 0 \\ 0 & \vec{R}_f & 0 \\ 0 & 0 & \vec{R}_d \end{pmatrix} \cdot \begin{pmatrix} \vec{I}_w \\ \vec{I}_f \\ I_d \end{pmatrix} + \begin{pmatrix} \vec{0} \\ \vec{V}_f \\ 0 \end{pmatrix}$$

- In the state-space form

$$\begin{aligned} \dot{\vec{x}} &= \vec{A}\vec{x} + \vec{B}\vec{u} \\ \vec{y} &= C\vec{x} \end{aligned}$$

where $\vec{x} = \begin{pmatrix} \vec{I}_w & \vec{I}_f & I_d \end{pmatrix}^T$; $\vec{A} = -\vec{L}^{-1} \cdot \vec{R}$; $\vec{B} = \vec{L}^{-1} \cdot \vec{I}_{cc}$; $\vec{u} = \vec{V}_f$

& measurements $\vec{y} = \vec{\Phi}_s$ are sensor fluxes

- Classical control law with proportional gain defined as $\vec{u} = -\vec{G}_p \vec{y}$

Balanced Truncation significantly reduces VALEN state-space

$$\begin{aligned}\dot{\vec{x}} &= \tilde{A}\vec{x} + \tilde{B}\vec{u} \\ \vec{y} &= C\vec{x}\end{aligned}$$

- Measure of system controllability and observability is given by controllability and observability grammians for stable Linear Time-Invariant (LTI) Systems

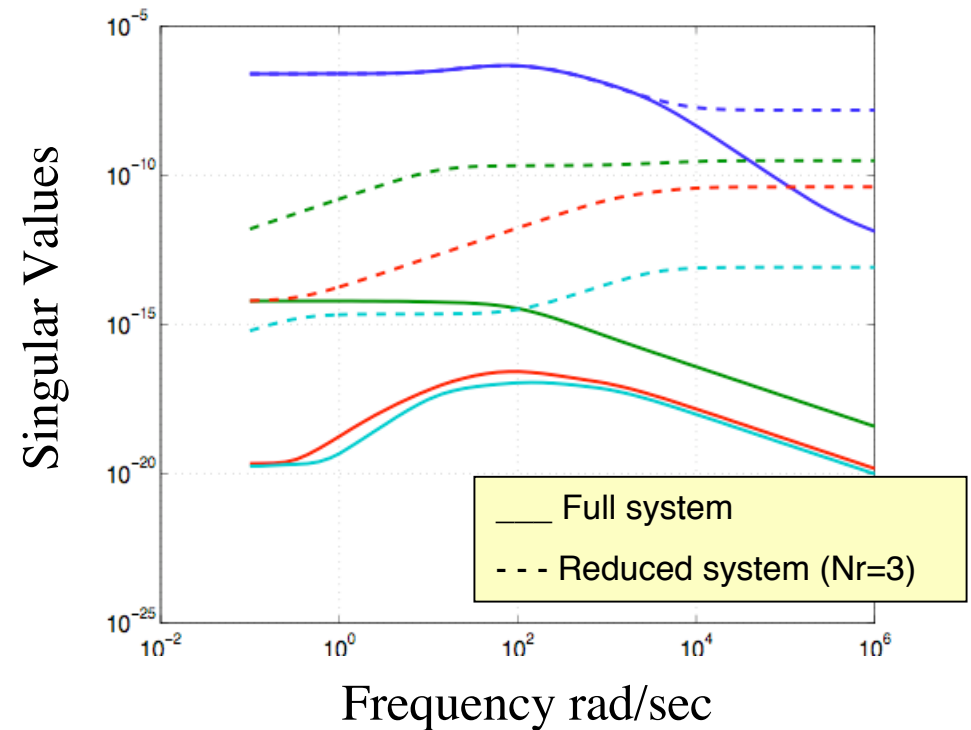
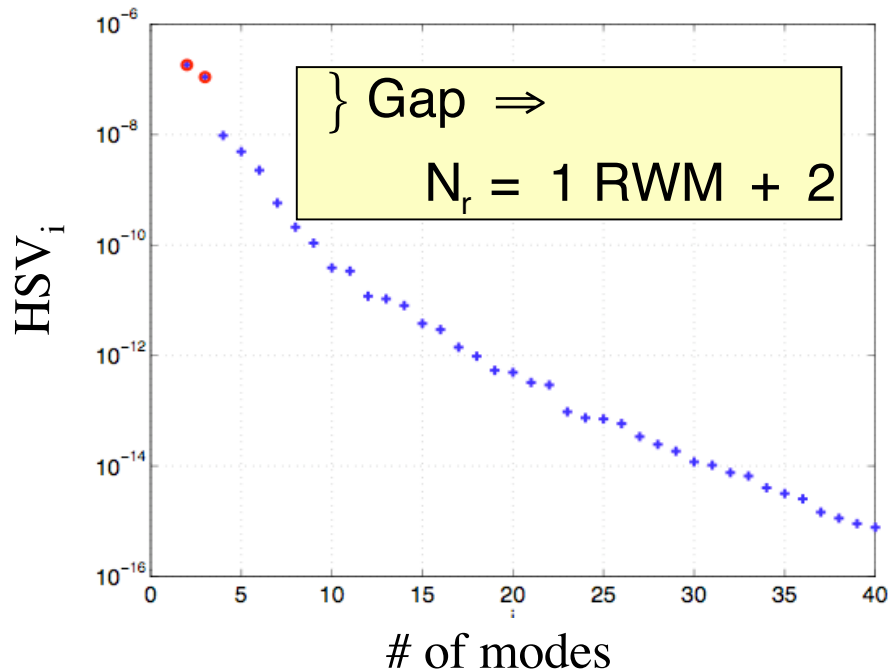
$$\Gamma_c = \int_0^\infty e^{A\tau} B B^T e^{A^T \tau} d\tau \quad \Gamma_o = \int_0^\infty e^{A^T \tau} C^T C e^{A\tau} d\tau$$

- Can be calculated by solving continuous-time Lyapunov equations:

$$A\Gamma_c + \Gamma_c A^T + B B^T = 0 \quad A^T \Gamma_o + \Gamma_o A + C^T C = 0$$

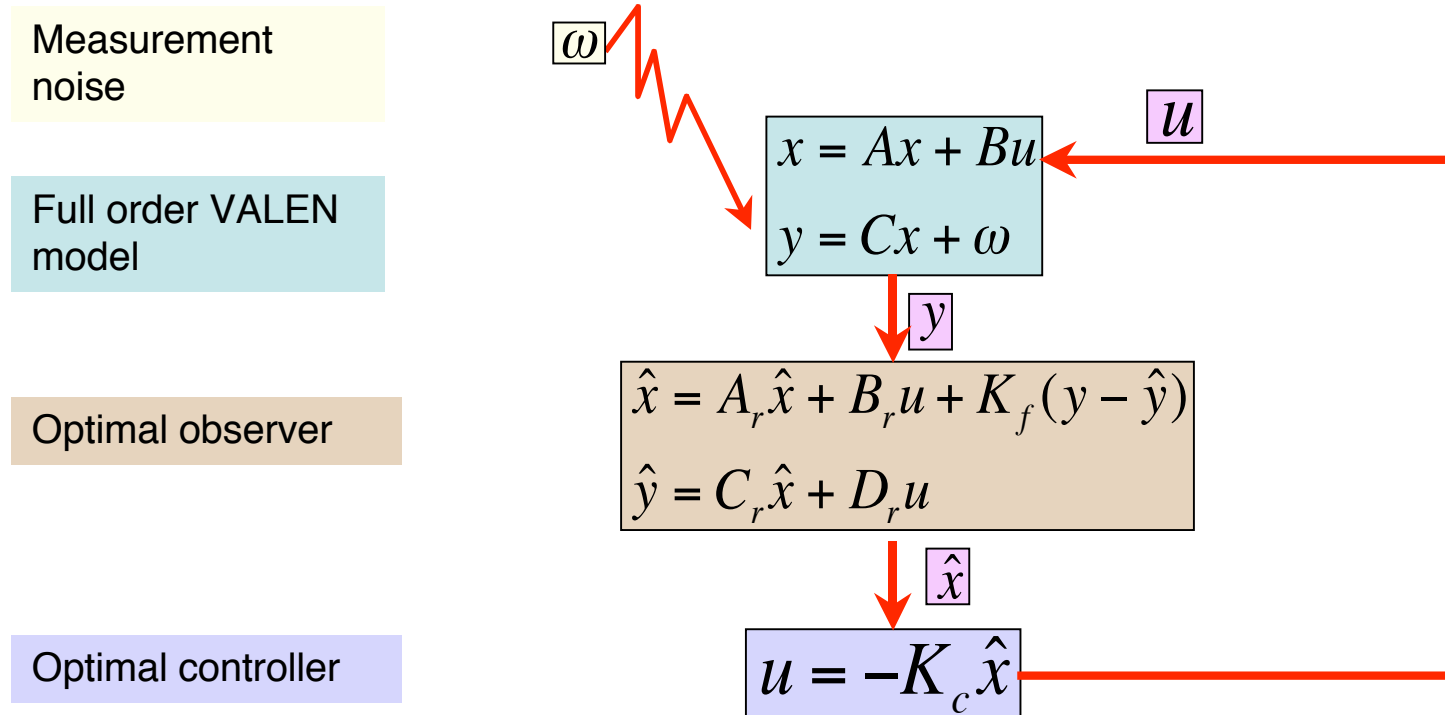
- Balanced realization exists for every controllable & observable system $\Gamma_c = \Gamma_o = \begin{pmatrix} \sigma_1 & 0 & 0 \\ 0 & \ddots & 0 \\ 0 & 0 & \sigma_n \end{pmatrix}, \quad \begin{matrix} \sigma_i > \sigma_j \\ \text{for } i > j \end{matrix}$
- Balanced truncation reduces VALEN state space from several thousand elements to ~15 or less $\vec{x} = (\vec{x}_1, \vec{x}_2)^T \quad \begin{pmatrix} \dot{\vec{x}}_1 \\ \dot{\vec{x}}_2 \end{pmatrix} = \begin{pmatrix} A_{11} & A_{12} \\ A_{21} & A_{22} \end{pmatrix} \begin{pmatrix} \vec{x}_1 \\ \vec{x}_2 \end{pmatrix} + \begin{pmatrix} B_1 \\ B_2 \end{pmatrix} \vec{u}$
 $\vec{y} = (C_1 \ C_2) \begin{pmatrix} \vec{x}_1 \\ \vec{x}_2 \end{pmatrix} + D\vec{u}$

HSV spectrum of KSTAR VALEN state-space suggests a reduction of stable part of the system to **just 2** balanced states



- LQG controller uses **4 central IVCC & 16 mid-plane poloidal sensors**
- Clear gap in HSV spectrum
- Largest SV includes the **full system frequency response up to an RWM passive growth rate.**

Closed System Equations with Optimal Controller and Optimal Observer based on Reduced Order Model



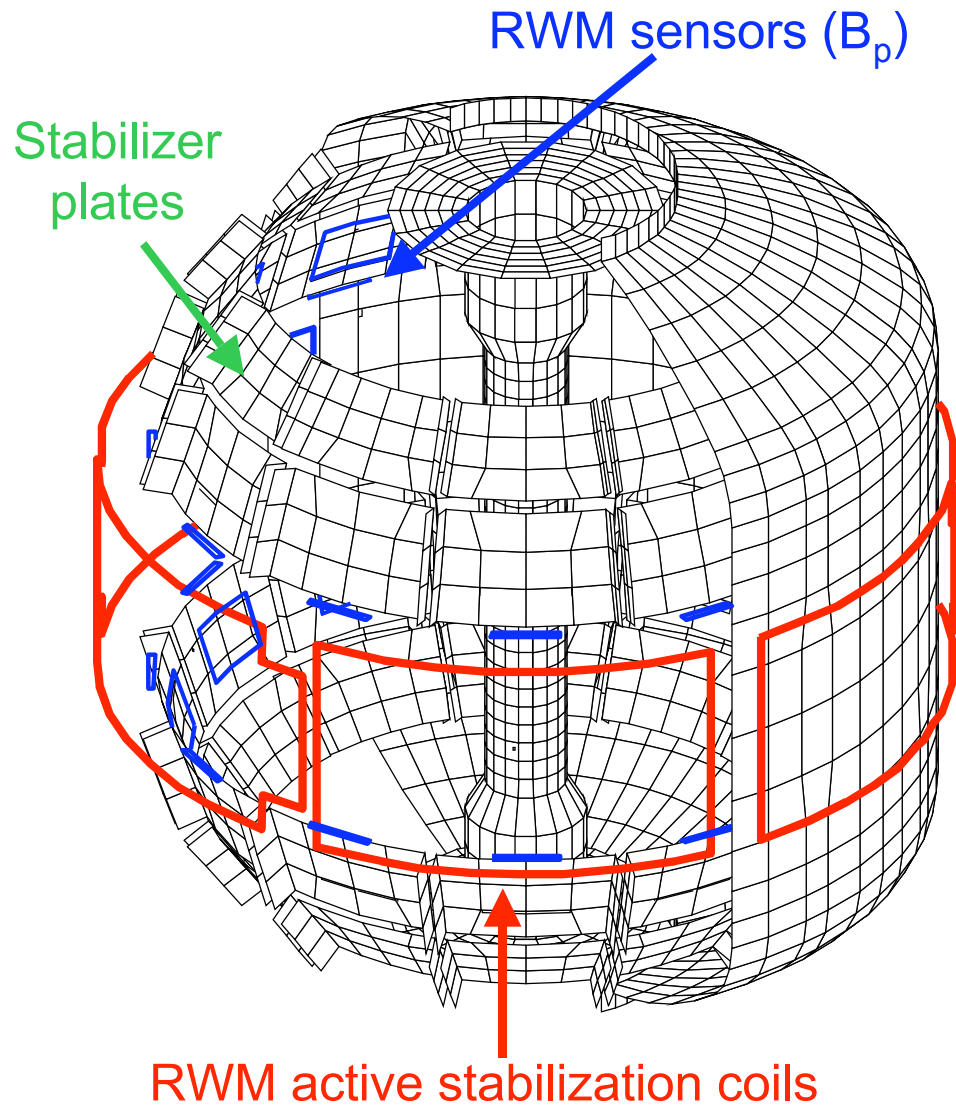
$$\begin{pmatrix} \dot{x} \\ \dot{\hat{x}} \end{pmatrix} = \begin{pmatrix} A & -BK_c C_r \\ K_f C & F \end{pmatrix} \begin{pmatrix} x \\ \hat{x} \end{pmatrix} + \begin{pmatrix} 0 \\ K_f \end{pmatrix} \omega$$

$$F = A_r - K_f C_r - (B_r - K_f D_r) K_c C_r$$

← Closed loop continuous system allows to

- ❑ Test if Optimal controller and observer stabilizes original full order model
- ❑ Verify robustness with respect to β_n
- ❑ Estimate RMS of steady-state currents, voltages and power

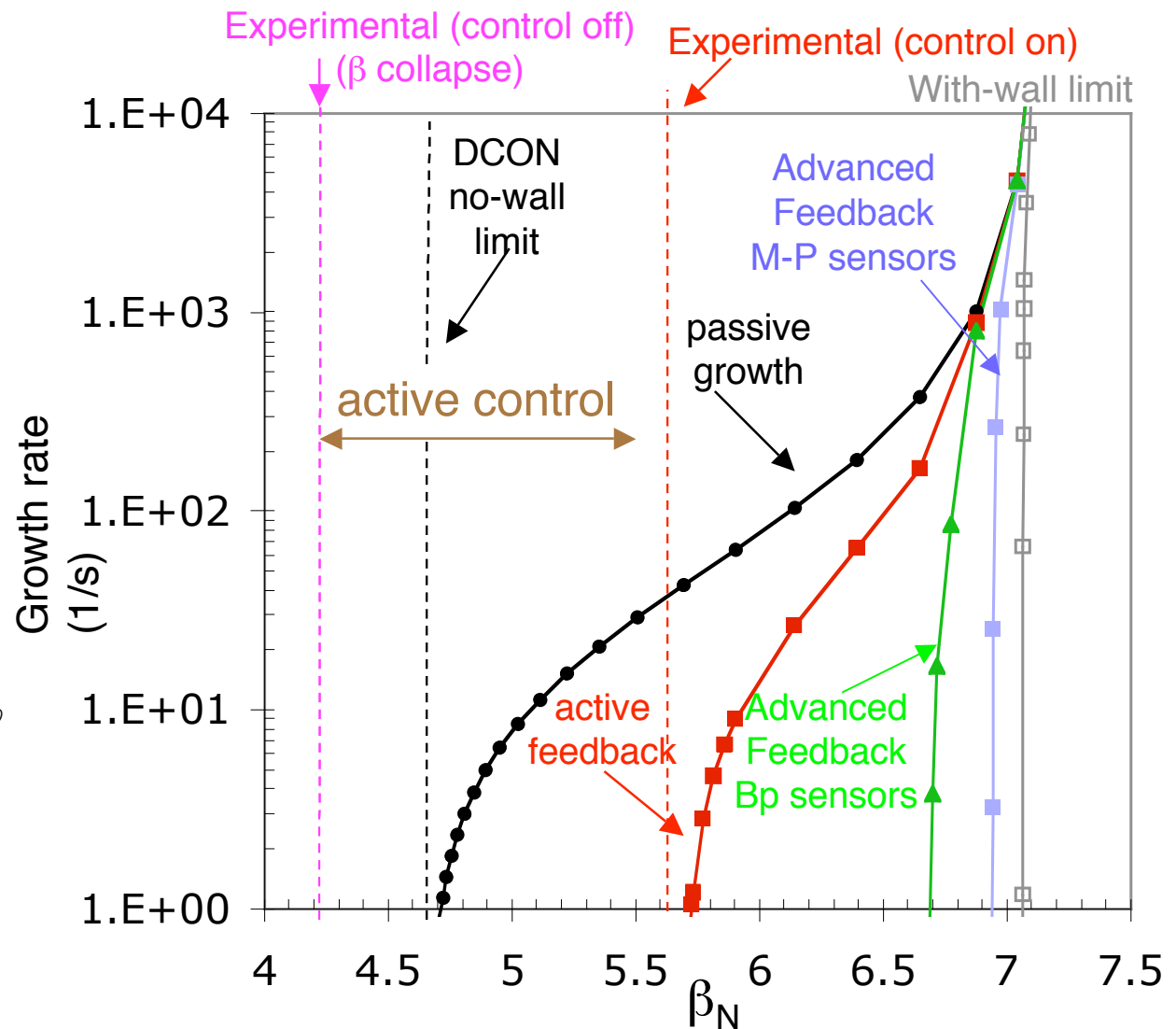
Advanced controller methods planned to be tested on **NSTX** with future application to KSTAR



- VALEN NSTX Model includes
 - ❑ Stabilizer plates for kink mode stabilization
 - ❑ External mid-plane control coils closely coupled to vacuum vessel
 - ❑ Upper B_p sensors in actual locations
 - ❑ Compensation of control field from sensors
 - ❑ Experimental Equilibrium reconstruction (including MSE data)
- Present control system on NSTX uses Proportional Gain

Advanced control techniques suggests significant feedback performance improvement for NSTX up to $\beta_n / \beta_n^{\text{wall}} = 95\%$

- Classical proportional feedback methods
 - ❑ VALEN modeling of feedback systems agrees with experimental results
 - ❑ RWM was stabilized up to $\beta_n = 5.6$ in experiment.
- Advanced feedback control may improve feedback performance
 - ❑ Optimized state-space controller can stabilize up to $C_\beta = 87\%$ for upper Bp sensors and up to $C_\beta = 95\%$ for mid-plane sensors
 - ❑ Uses only 15 modes for optimal observer and controller design



Next steps and future work on the KSTAR stability analysis

- Expand equilibrium / ideal stability analysis as needed
 - ❑ Collaborate on equilibrium reconstructions of first plasmas
- Closer definition of RWM control system circuit by interaction with KSTAR engineering team
- Improved noise model for KSTAR sensor noise
- LQG controller with plasma rotation for KSTAR
- LQG controller tests on NSTX with application to KSTAR RWM control system design
- Critical latency testing for KSTAR RWM control

KSTAR is capable of producing long-pulse, high β_n stability research

- Machine designed to run high β_n plasmas with low I_i and significant plasma shaping capability
- Large wall-stabilized region to kink/ballooning modes with $\beta_n / \beta_n^{\text{no-wall}} = 2$ at highest β_n predicted for the device
 - Co-directed NBI, passive stabilizers allow kink stabilization
- Active IVCC mode control system provide strong RWM control
 - IVCC design allows active $n=1$ RWM stabilization at very high $C_\beta > 98\%$
- Fast IVCC circuit for stabilization is possible at reasonable power levels

Optimal controller and observer based on reduced order VALEN model reduce power and achieve higher β_n

Controller: $u = -K_c \hat{x}$

Minimize Performance Index: $J = \int_t^T \left(\hat{x}'(\tau) Q_r(\tau) \hat{x}(\tau) + \vec{u}'(\tau) R_r(\tau) \vec{u}(\tau) \right) d\tau \rightarrow \min$
 Q_r, R_r - state and control weighting matrix,

Controller gain for the steady-state can be calculated as $K_c = R^{-1} B_r^T S$

where S is solution of the controller

Riccati equation

$$S A_r + A_r^T S - S B_r R_r^{-1} B_r^T S + Q_r = 0$$

Observer: $\dot{\hat{x}} = A_r \hat{x} + B_r u + K_f (y - C_r \hat{x})$

Minimize error covariance matrix

$$E \left\{ (x - \hat{x})(x - \hat{x})^T \mid y(\tau), \tau \leq t \right\} \rightarrow \min$$

where $K_f = P C^T W^{-1}$ is Kalman Filter gain and

P is solution of observer

Riccati equation

$$A_r P + P A_r^T - P C_r^T W^{-1} C_r P + V^T = 0$$

V, W plant and measurement noise covariance matrix.

Noise on RWM sensors sets control system power

- Gaussian white noise

- ~1.5Gauss RMS, based on noise in DIII-D RWM B_p sensors
- Minimum estimate of control power consumption
 - Perfect response to RWM
 - No other coherent modes

- Experimental sensor input

- NSTX B_p sensor during RWM active stabilization
- Maximum estimate of control system power consumption
 - DC offset from resonant field amplification; stray field from passive plate currents
 - The $\Delta B/B_0$ larger in ST than at higher aspect ratio

